Catalysis Today 175 (2011) 568–575

Contents lists available at ScienceDirect

Catalysis Today

journal homepage: www.elsevier.com/locate/cattod

Mesoporous titania with high crystallinity during synthesis by dual template system as an efficient photocatalyst

Sajjad Shamaila, Ahmed Khan Leghari Sajjad, Feng Chen, Jinlong Zhang*

Key Lab for Advanced Materials and Institute of Fine Chemicals, East China University of Science and Technology, 130 Meilong Road, Shanghai 200237, PR China

ARTICLE INFO

Article history:
Received 28 September 2010
Received in revised form 18 February 2011
Accepted 16 March 2011
Available online 27 April 2011

Keywords:
Mesoporous titania
Dual templates
High crystallinity
Phenol
Mineralization

ABSTRACT

The mesoporous titania, designated MS-TiO_2 was successfully prepared via a new combination of pluronic P123 and poly ethylene glycol templates and acetic acid as the hydrolytic retardant with extremely high crystallinity achieved during synthesis process. MS-TiO_2 has remarkable thermal stability, biporous mesostructure and superior photocatalytical activity for phenol degradation and mineralization as compared to mesoporous TiO_2 prepared using single template systems. The anatase–rutile phase transformation of the MS-TiO_2 was not observed up to 800 °C. The mesoscale order of MS-TiO_2 was retained after thermal treatment up to 450 °C as confirmed by low angle X-ray diffraction and transmission electron microscopy analyses. It maintained its pore properties at high temperature of 700 °C with a significant pore size 10.4 nm and pore volume 0.11 cm^3/g. MS-TiO_2 has biporous mesostructure with the small mesopore of 5.5 nm and the large mesopore of 8.7 nm in mean pore diameters. The MS-TiO_2 showed higher photocatalytic activity for phenol degradation than mesoporous titania prepared using single templates and standard system of Degussa P25. The remarkably high catalytic activity of the MS-TiO_2 is attributed to its high crystallinity and biporous mesostructure. The phenol mineralization was confirmed using high performance liquid chromatography and total organic carbon analyses.

1. Introduction

Functional metal oxide material, has been a hot topic of interest due to enormous application potentials of such materials as membranes, in catalysis, solar energy conversion and as chemical sensors [1–8]. Among these, mesoporous titania is of particular interest since this class of materials possesses well-defined porosity and large specific surface areas [9,10]. For photocatalytic degradation of organics, these desirable properties are anticipated to improve the photocatalytic activity. However, it is quite difficult to fabricate mesoporous titania with an anatase crystalline wall during the synthesis process with thermal stability. The relatively low thermal stability of the titania based mesoporous materials is often attributed to their phase transformation and pore shrinkage derived from elimination of the structure-directing agents and the wall is too thin to retain the mesoporous structure during crystallization [11,12]. From a viewpoint of catalytic application, it is very significant to synthesize the mesoporous titania with high crystallinity and thermal stability.

Many reports focused on synthesis of mesoporous TiO_2 using costly titanium alkoxide or inorganic reagent as a Ti source, which was prepared via complex physicochemical process. The obtained mesoporous TiO_2 was usually an amorphous or poor anatase phase with poor thermal stability. The ideal material would be porous, highly crystalline and present a high surface-to-volume ratio to enhance exchange with a second phase or the environment. In the past, copolymer-directed TiO_2 synthesis has typically been limited to temperature treatments below 400 °C to prevent collapse of the mesoporous structure. The resulting limited crystallinity of TiO_2 annealed at these relatively low temperatures is thought to contribute towards its low electron diffusion coefficient due to a high density of trap sites. The combination of high temperature treatment while maintaining a high porosity has been demonstrated by Lee et al. [13] employing a combined assembly of soft and hard chemistries method. Recently, Yoshitake et al. [14] improved thermal stability of template (primary amine)-extracted titania through CVD treatment of titanium isopropoxide. Cassiers et al. [15] synthesized NH_3-treated titania, which was stable up to 600 °C.

The other approach is to use dual or multiple templates in different ranges to produce hierarchical pore structure. For the mesopores, the supramolecular arrays of amphiphilic block copolymers [16–18] or other surfactants are commonly used as templates, through which the materials exhibit a narrow pore size distribution. There are some reports about the use of dual template systems. Holland et al. [19] used arrays of monodiperse polystyrene spheres as templates for macropores and tetrapropylammonium hydroxide for mesopores. Sen et al. [20] synthesized silica materials with macro–meso–microporous structure using polystyrene spheres, F127 and P123 as templates, respectively. Sun et al. [21] presented a two-step route to produce bimodal pore structure. Firstly, MCM-41

* Corresponding author. Tel.: +86 21 64252062; fax: +86 21 64252062.
E-mail address: jlzhang@ecust.edu.cn (J. Zhang).

0920-5861/$ – see front matter © 2011 Elsevier B.V. All rights reserved.
doi:10.1016/j.cattod.2011.03.041

nanoparticles were prepared, using CTAB as mesopore templates. Then the nanoparticles were cross-linked around assemblies of triblock copolymer to produce macroporous structure. Groenewolt et al. [22] prepared silica monoliths with bimodal pore structure by nanocasting mixtures of fluorinated nonionic surfactants and micelles of two hydrocarbon block copolymers. Micelles with different sizes formed by different surfactants acted as the templates for hierarchical pore structure. Sheng et al. [23] synthesize biporous TiO_2 using a double surfactant system of F127 and DDA (Dodecylamine). Smatt et al. [24] designed a dual-templating route to synthesize silica monoliths. PEG and CTAB were utilized as templates for macropores and mesopores, respectively.

In the present work we employed a new combination of templates of pluronic P123 (P123) and poly ethylene glycol (PEG) and acetic acid (Hac) as hydrolytic retardant for the preparation of mesoporous titania. Mesoporous TiO_2 prepared using dual tempalates materials (MS-TiO_2) exhibited high crystallinity with a nanocrystalline anatase structure in the as-synthesized state, remarkable thermal stability and biporous mesopore structure. This new dual template system proved a valuable combination for the preparation of mesoporous anatase with special characteristics as compared to mesoporous TiO_2 prepared using single template systems. MS-TiO_2 showed the superior catalytic activity for phenol degradation and mineralization as compared to the standard system of Degussa P25 and mesoporous TiO_2 prepared using single template systems.

2. Experimental

2.1. Materials

Tetrabutyl titanate (TBT) $Ti(OBu)_4$, PEG with the molecular weight of 600 (designated as PEG600), absolute ethanol and acetic acid (Hac) were analytical grade. Pluronic P123 [(M_w) 5800, $HO–(CH_2CH_2O)_{20}(CH_2–CHCH_3O)_{70}(CH_2CH_2O)_{20}H$, $EO_{20}PO_{70}EO_{20}$, abbreviated as P123], was purchased from Aldrich. P25 (a commercial nanocrystalline TiO_2 that consists of ca. 80% anatase and 20% rutile; BET area ca. 50.0 $m^2\,g^{-1}$) was supplied by Degussa. All the above chemicals were purchased from Shanghai Sinopharm Chemical Reagent Co., Ltd., China. Double-distilled water was used throughout the experiments.

2.2. Catalyst preparation

In a typical synthesis procedure, 5.0 g of TBT was added drop-by-drop to 30 mL of Hac aqueous solution (20%, v/v) under vigorous stirring. The mixed solution was sealed and stirred continuously for 4 h to obtain solution A. In a separate beaker, 3.0 g of PEG 600 and 1.0 g of P123 was dissolved in 20 mL ethanol under vigorous stirring to obtain solution B. Solution B was then added drop-by-drop to solution A. The final mixed solution was sealed and stirred for 24 h at room temperature. The resultant solution was then transferred into a Teflon sealed container for hydrothermal treatment under a constant temperature of 120 °C for 48 h. The precipitations were then collected and dried overnight in air at 80 °C. The as-prepared sample was then subjected to a thermal treatment process at 450 °C for 4 h. As-prepared sample was calcined at different temperatures as well. Furthermore, in order to evaluate the effect of the use of dual template system we replaced the dual template system with single template P123 and PEG.

2.3. Characterization

The crystal phase composition and crystallinity of the obtained mesoporous-TiO_2 was determined by X-ray diffraction (XRD). X-ray diffraction patterns of all samples were collected in the range 10–80° (2θ) for wide angle XRD and 0.5–8° (2θ) for small angle XRD using a Rigaku D/MAX 2550 diffractometer (Cu $K\alpha_1$ radiation, λ = 1.5406 Å), operated at 40 kV and 100–200 mA. The crystallite size was estimated by applying the Scherrer equation to the full width at half-maximum (fwhm) of the (1 0 1) peak of anatase. $D = k\lambda/\beta\cos\theta$, where β is the half-height width of the diffraction peak of anatase, K = 0.89 is a coefficient, θ is the diffraction angle and λ is the X-ray wavelength corresponding to the Cu Kα irradiation. The morphology was studied using transmission electron microscopy (TEM, JEOL JEM-2011) with an accelerating voltage of 200 kV. Nitrogen adsorption and desorption isotherms were obtained at 77 K with a Micromeritics ASAP 2010 system. All the samples were degassed at 473 K before the measurement. TGA/DTA was performed on the Perkin Elmer Pyris Diamond thermo gravimetric analyzer.

2.4. Photocatalytic activity test

The photocatalytic activity was evaluated in terms of the degradation of phenol. Phenol was chosen as a model pollutant to evaluate the photocatalytic activities. The photocatalytic reactions were carried out at 30 °C using a home-made reactor. 300 W high-pressure Hg lamp having strongest emission wavelength of 365 nm was used as a UV light source (the average light intensity was about 1230 $\mu W\,cm^{-2}$), mounted 10 cm away from the reaction solution. The photocatalyst (0.05 g) was added into a 100 mL quartz photo reactor containing 50 mL of a 40 $mg\,L^{-1}$ aqueous solution of phenol. The mixture was sonicated for 5 min and stirred for 30 min in the dark in order to reach the adsorption–desorption equilibrium. Under UV irradiation and vigorous stir, each reaction was lasted for 5 h. Preliminary studies indicated a linear light absorbance verse phenol concentration and that the decomposition of phenol in the absence of photocatalyst or UV irradiation could be neglected. The reproducibility was checked by repeating the measurements at least three times and was found to be within the acceptable limit (±3%).

To analyze the concentration of phenol and degradation products, the suspension was first centrifuged and filtered through 0.22 μm Millipore membrane filters to remove the catalyst. The concentrations of phenol were measured with a UV–vis spectrophotometer (Varian Cary 100) with UV absorbance in the range of 200–400 nm, and the absorbance at 269 nm corresponded to the maximal adsorption of phenol. The concentrations of phenol were calculated from the height of peak using calibration curve. The decrease of total organic carbon (TOC), which indicated the mineralization of phenol, was determined using an Elementar TOC analyzer.

Phenol degradation intermediates were determined by the HPLC series 1100 (Agilent) is equipped with a reverse-phase C18 analytical column (Zorbax SB-C18, USA) of 150 mm × 2.1 mm and 3.5 μm particle diameter. Column temperature was maintained at 22 °C. The mobile phase used for eluting phenol from the HPLC columns consisted of acetonitrile and water (30:70 v/v) at a flow-rate of 0.3 $mL\,min^{-1}$.

3. Results and discussion

In this procedure, we employ a new combination of template system of P123 and PEG with acetic acid. Acetic acid acts as the hydrolytic retardant, for better control of the hydrolysis process of titanium sources due to the chelating effect of acetic anions and formation of pH buffer [25–27]. In the new dual-template system the PEG affects the formation of the mesopore structure by changing the micelle size of P123. The addition of PEG enlarged the mesopore size and widened the mesopore size distribution of the material, it

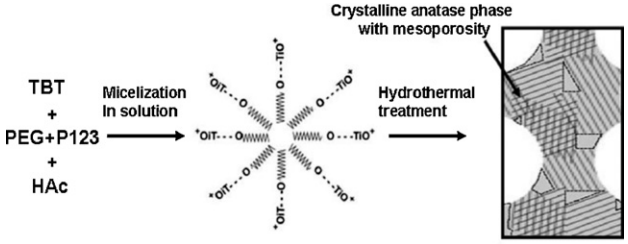

Scheme 1. Proposed mechanism of as prepared MS-TiO_2 sample.

co-micellized with P123 and stabilized hydrophilic–hydrophobic interface. The micelles of these block copolymers possess a higher hydrophobic contrast than only pluronic [28] or PEG type copolymers (the standard system), thus leading to a greater driving force for self-assembly. The long hydrophobic chain offers the possibility of synthesizing mesoporous oxides with thick walls that may lead to an increased thermal stability. The composite surfactants give a unique combination as compared to single template [29,30] and cooperatively self assemble to facilitate the mesoporous structure by inducing hydrolysis of TBT solution and to obtain thicker titania framework leading to high crystallinity and thermal stability of the mesoporous titania prepared using dual tempalates. Thus give the highly crystalline anatase in as prepared form.

In this system anatase is formed during the synthesis process before calcinations. The moment of anatase formation depends on both medium and type of surfactants used, because the condensation rate of titania is influenced by the medium used and nature of surfactants. In acidic medium, titania is positively charged, because the pH is lower than the isoelectric point of titania. When the ethanolic solution of templates is added in the acidic acetic acid solution of TBT, the templates formed a strong interaction with titania which results in the less strong interaction between neighboring titania particles leading to less condensed state of mesostructured titania. Subsequently the hydrothermal treatment can condensate the titania particles into an anatase containing mesoporous structure as represented in Scheme 1.

3.1. Thermogravimetric analysis (TGA/DTA)

Thermogravimetric analysis (TGA/DTA) was performed for the as synthesized MS-TiO_2 sample to replicate the calcination conditions as shown in Fig. 1. The analysis was carried out at a heating rate of 10 °C/min from 40 to 800 °C in air. Below 200 °C, 3.2% mass loss was due to volatile species (water, ethanol, acetic acid) [18,31]. Between 200 and 400 °C, a mass loss of 16.8% was raised due to the decomposition of the templates. Some residual organic matter, such as amorphous carbon or carboxylate species and possibly hydroxyl groups, was removed at temperatures between 400 and 450 °C with a mass loss of 2.5%. Above 450 °C the mass loss was negligible. There is a slight weight gain above 720 °C. This weight gain between 720 and 800 °C is only about 1.0% which could be due to the change in buoyancy as the density of the purge gas decreases with temperature. Based on this TGA trace and several related papers [31,32], the as synthesized samples were calcined at 450 °C for 4 h for complete removal of templates from the thermally stable mesoporous titania.

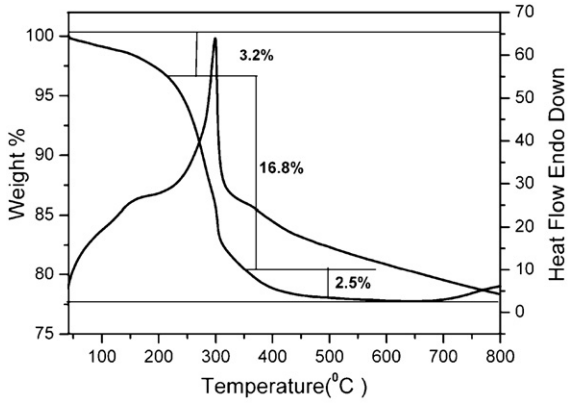

Fig. 1. TGA/DTA of as prepared MS-TiO_2.

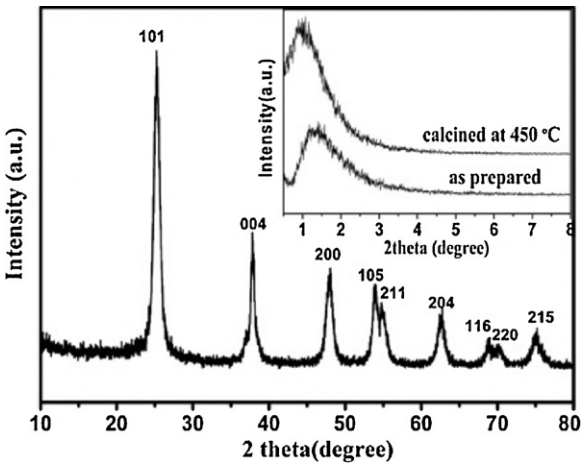

Fig. 2. Wide angle X-ray diffraction patterns of MS-TiO_2 as prepared. Inset the small-angle X-ray diffraction patterns of MS-TiO_2 as prepared and calcined at 450 °C.

3.2. X-ray diffraction (XRD)

The small-angle X-ray diffraction (SAXRD) patterns of the MS-TiO_2 as prepared and calcined at 450 °C show one high-intensity peak as represented in inset of Fig. 2. With calcination the diffraction peak shifts to the lower angle which corresponds to the *d*-spacing increase. A clear retention of the diffraction line can be observed for MS-TiO_2 up to a calcination temperature of 450 °C, which is not possible without the use of dual template system. Whereas mesoporous TiO_2 prepared using single template the as prepared samples show small angle diffraction which totally disappear at 450 °C due to the collapse of the mesoporous structure as represent in inset of Fig. 3a and b.

The wide angle X-ray diffraction (WAXRD) patterns obtained from samples by dual and single template systems are shown in Figs. 2, 3a and b, respectively. These samples exhibit characteristic anatase peaks, which can be indexed to 25.3 (1 0 1), 37.2 (0 0 4), 48.9 (2 0 0), 54.0 (1 0 5), 55.3 (2 1 1), 62.4 (2 0 4) and 68.7° (1 1 6) (JCPDS no. 21-1272). As prepared sample also shows the high intensity anatase peaks which suggest that anatase is the highly crystalline phase in the sample after preparation. This confirms that Ti sol originating from acetic acid and new dual template system can lead to better crystallized anatase titanium dioxide. This might be due to the benefits of replacing strong acid with dilute acetic acid. When HCl was used in place of acetic acid the obtained mesoporous titania is amorphous before hydrothermal treatment and show lower crystallinity of anatase as compared to mesoporous titania prepared using acetic acid as shown in Fig. 4. It is well known that the titanium precursor rapidly hydrolyzed in strong acid (HCl) media often leads to the aggregation and formation of large size particles because of uncontrollable hydrolysis causes by the rapid pH change [27,33,34].

The mean crystal sizes calculated by Scherrer equation of MS-TiO_2 and mesoporous TiO_2 prepared using single template P123

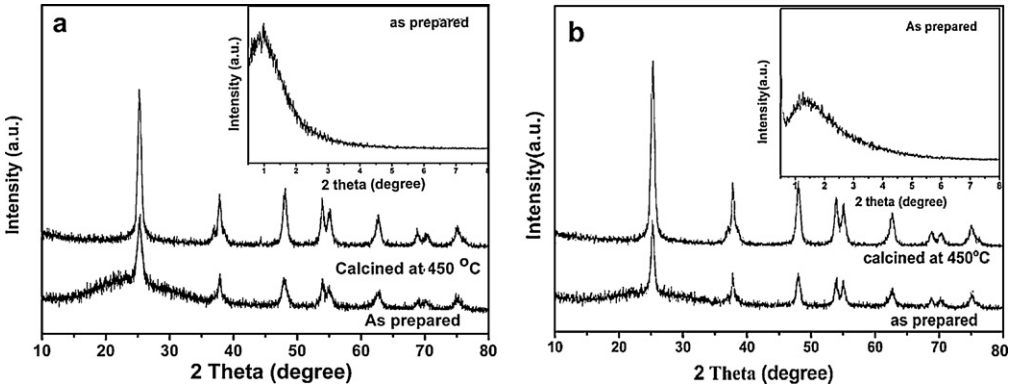

Fig. 3. The wide angle X-ray diffraction pattern of mesoporous-TiO_2 prepared (a) using PEG and (b) using P123 as single template. Inset small angle X-ray diffraction pattern of as prepared samples.

and PEG calcined at 450 °C was 12.8, 13.7 and 14.0 nm, respectively [35]. When the as prepared samples were calcined up to 800 °C, the mean crystal size of MS-TiO_2 samples increased from 9.0 to 38.1 nm.

3.3. Thermal stability

The crystal structure of TiO_2 depends on the temperature of heat treatment. It is commonly considered that the anatase phase of TiO_2 shows better photocatalytic activity than the rutile one. Fig. 5 shows high crystallinity with a nanocrystalline anatase structure even in the as-synthesize state. When the samples are calcined, the peak width and the intensity of anatase phase at $2\theta = 25.3^\circ$ become more strong and sharp which indicate the formation of larger crystallite size and higher crystallinity. Anatase TiO_2 can be obtained from not only the as-prepared sample but also those samples even heated up to 800 °C for 2 h, during which no rutile phase is observed as illustrated in Fig. 5a–f. When the catalyst is calcined at 900 °C, anatase–rutile phase transformation is observed in the titania sample. The anatase (1 0 1) peak at $2\theta = 25.3^\circ$ and the rutile (1 1 0) peak at $2\theta = 27.6$ are analyzed using the formula in order to estimate the anatase–rutile ratio of TiO_2 samples:

$$X_R = \left(1 + 0.8\frac{I_A}{I_R}\right)^{-1}$$

where X_R is the weight fraction of rutile in the powders and I_A and I_R are the XRD peak intensities of the anatase and rutile phases, respectively. When the samples of MS-TiO_2 are calcined at 900 °C, 70% anatase TiO_2 is transformed to rutile phase (Fig. 5g) while the samples prepared with single templates show this transformation at 700 °C. The results reveal that the present preparation is unique in producing anatase TiO_2 sample with considerably high resistant to the phase transformation to rutile. In our synthetic method, the thermal stability of the mesoporous titania is extremely high because the as prepared anatase was highly crystalline after hydrothermal treatment. Moreover, the dual template system, successfully maintained the distance between the anatase clusters incorporated into the mesopores and maintain its high pore properties at high temperature resulting in the suppression of the anatase–rutile phase transformation up to 800 °C.

3.4. N_2 sorption data

The pore size distributions and N_2 sorption isotherms of the MS-TiO_2 in comparison with mesoporous TiO_2 prepared by single template system at 450 °C calcination temperature are given in Fig. 6. All the samples display similar nitrogen sorption isotherms. These isotherms exhibit a Type IV adsorption/desorption shape with a H_2 hysteresis loop, at high relative pressure range between 0.4 and 0.8 indicating the abundance of mesopores in samples. The isotherm of the MS-TiO_2 shows two major capillary condensation steps representing the two types of mesopores inside the titania particles. MS-TiO_2 exhibits biporous mesostructure with pore sizes of 5.5 and 8.7 nm while the mesoporous TiO_2 using single template P123 and PEG show the pore sizes of 6.3 and 6.8 nm, respectively. Up to 700 °C, the porous structure of the MS-TiO_2 is

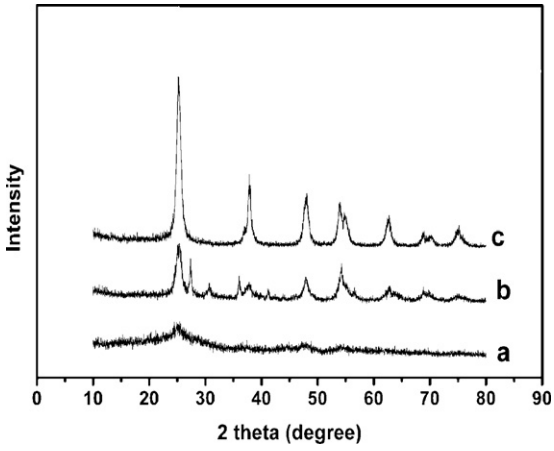

Fig. 4. The wide angle X-ray diffraction patterns for as prepared samples (a) using HCl without hydrothermal treatment, (b) using HCl with hydrothermal treatment and (c) MS-TiO_2 prepared by acetic acid with hydrothermal treatment.

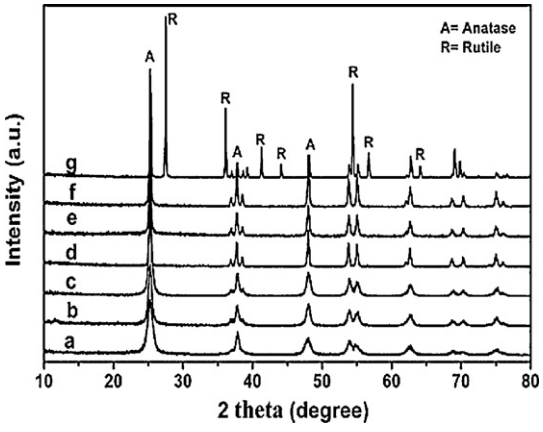

Fig. 5. MS-TiO_2 calcined at different calcination temperatures (a) as prepared, (b) 450 °C, (c) 500 °C, (d) 600 °C, (e) 700 °C, (f) 800 °C and (g) 900 °C.

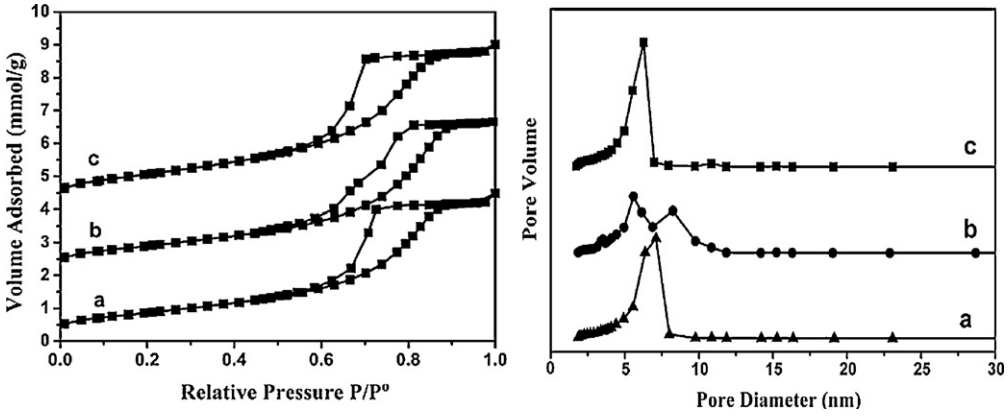

Fig. 6. Pore size distributions and N_2 adsorption/desorption isotherms of mesoporous TiO_2 calcined at 450 °C (a) with single template PEG, (b) MS-TiO_2 prepared by combination of templates PEG and P123 and (c) with single template P123.

maintained as shown in Table 1. The pore volume is sustained in the range of 0.24–0.11 cm^3/g in the calcination range of 450–700 °C. Detailed pore structure properties are listed in Table 1. Generally, the anatase is transformed into rutile by thermal treatment in the temperature range of 600–700 °C [36] resulting in the mesostructure collapse of the mesoporous titania along with a significant decrease in pore properties such as specific surface area and pore volume [37–39]. In contrast, the MS-TiO_2 has the stable anatase crystal up to 800 °C, resulting in the maintenance of its high pore properties at high temperature.

3.5. Transmission electron microscopy

Transmission electron microscopy (TEM) images of the MS-TiO_2 in Figs. 7a and 8a reveal that the titania particles are uniform, rounded and rectangular shape with pores in interstitial spaces between anatase particles, with anatase crystalline nanodomains of about 12–13 nm in size. These results correspond well with the domain size (ca. 12 nm) obtain from XRD. The single broad SAXRD peak of the TiO_2 at 450 °C (Fig. 2 inset), indicating no discernible order of the pore arrangement in long range [40] is in consistent with the TEM micrograph. Such disordered structure can actually be explained by the interactions between the titanium source and the mesopore templates. The multivalent Ti species can associate preferentially with the hydrophilic polyethylene oxide moieties mediated by PEG and P123 to form crown-ether-type complexes through coordination bonds by the self-assembly of the resulting complexes according to mesoscopic ordering, directed principally by the microphase separation of the block copolymer species. If a larger Ti oligomer or cluster linked with a PEO segment is formed in hydrolysis and condensation, this self-assembly for orderliness would be obstructed. This leads to a converse action for forming ordered mesostructure. The corresponding well-defined selected-area electron diffraction pattern in Fig. 7b of the MS-TiO_2 is also indicative of high anatase phase nanocrystallinity [13]. In Fig. 7c, the presence of clearly resolved lattice fringes demonstrates that the framework of the mesopores is composed of anatase nanocrystals. Thus HRTEM and XRD indicated the presence of mesopore network with a highly crystalline matrix between the mesopores. Mesoporous TiO_2 prepared using single template indicate a collapse of the mesopore structure as shown in Fig. 8b and c and confirmed by disappearance of SAXRD peak at 450 °C as shown in inset of Fig. 3a and b.

3.6. Photocatalytic activities

The photo degradation of phenol is employed to evaluate the photocatalytic activities of MS-TiO_2 and the mesoporous titania prepared with single template. No detectable degradation of phenol was observed without TiO_2 as the catalyst. For all three TiO_2 samples, adsorption was below 4.0% over the initial 1 h pre-equilibration period carried out in the dark, indicating that adsorption did not contribute considerably to the observed phenol removal. It was observed that these unique nanoparticles prepared by use of dual template system showed highest activity in the degradation of phenol. Degradation profile of phenol by MS-TiO_2 in comparison with samples by single templates and Degussa P25 is given in Fig. 9. It shows that after 5 h of irradiation, near complete degradation of phenol is observed with MS-TiO_2. Mesoporous TiO_2 prepared by use of single template P123 and PEG show 68.0%

Table 1
Structural parameters of mesoporous TiO_2 prepared using single templates and MS-TiO_2 prepared by dual template system under different calcination temperatures.

Samples	Calcination temperature (°C)	Particle size[a] (nm)	Surface area[b] ($m^2\ g^{-1}$)	Mean pore size[c]	Pore volume[d] (cm^3/g)
MS-TiO_2	450	12.0	87	5.5, 8.7	0.22
MS-TiO_2	550	17.0	70	9.3	0.18
MS-TiO_2	600	24.4	52	10.0	0.14
MS-TiO_2	700	32.6	45	10.4	0.11
With p123	450	13.7	73	6.3	0.18
With p123	550	17.8	42	10.1	0.11
With p123	650	34.5	9	15.9	0.01
With PEG	450	14.0	71	6.7	0.17
With PEG	550	18.2	40	10.7	0.10
With PEG	650	36.3	7	16.7	0.01

[a] Calculated by the Scherrer equation.
[b] BET surface area calculated from the linear part of the BET plot.
[c] Estimated using the desorption branch of the isotherm.
[d] Estimated by BJH method.

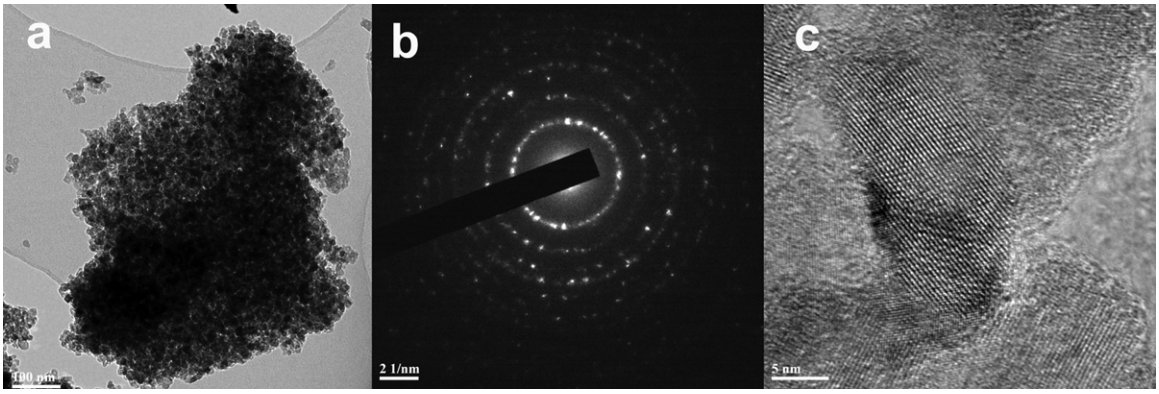

Fig. 7. (a) TEM image, (b) SAED and (c) HRTEM of MS-TiO_2 calcined at 450 °C.

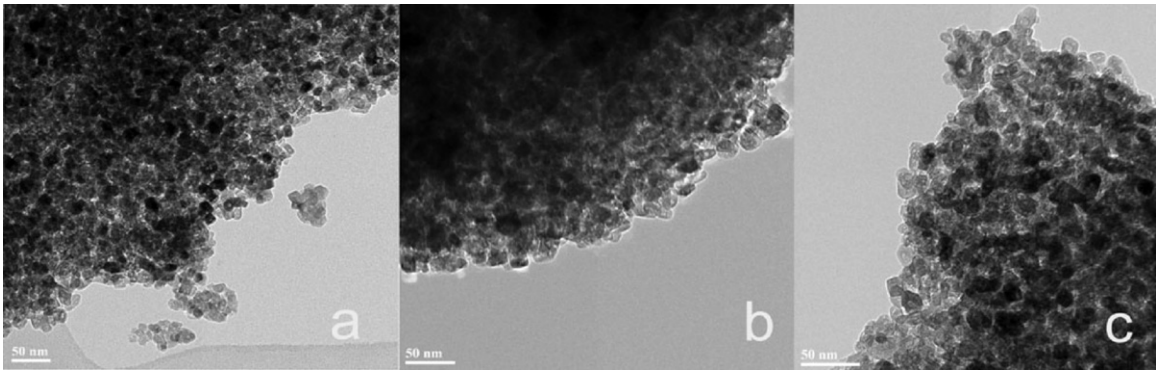

Fig. 8. TEM images of mesoporous TiO_2 (a) MS-TiO_2 with dual template (P123 + PEG), (b) with single template PEG and (c) with single template P123 calcined at 450 °C.

and 60.0% degradation, respectively, while the Degussa P25 shows only 40.0% of degradation under these experimental conditions. The photocatalytic activity of the MS-TiO_2 prepared by a combination of templates is far superior than that of the mesoporous TiO_2 prepared using single templates and Degussa P25. The increase in the photocatalytic efficiencies of MS-TiO_2 as compared to the mesoporous TiO_2 prepared using single templates and Degussa P25 is attributed to the high crystallinity of synthesized mesoporous-TiO_2 and the increased mesoporous parameters such as the mean pore size, BET surface area and the pore volume (Table 1).

Fig. 10 shows spectral changes during degradation of phenol, no new absorbance peaks are appeared after 5 h irradiations, indicating near complete degradation of phenol. The mineralization of phenol is confirmed by TOC and HPLC analysis as given in Figs. 11 and 12, respectively. TOC is decreased more quickly in the reaction using MS-TiO_2 as the catalyst (94% in 5 h). It suggests that phenol degradation and mineralization is even more completed. The degradation of phenol with effect of calcination temperature is presented in Fig. 13. The highest phenol degradation efficiency is observed at 450 °C and then decreased when the sample calcination temperature further increased up to 700 °C. This decrease of photocatalytic activity with calcination temperature is due to the collapse of mesopores and decrease of surface area as appeared in Table 1. MS-TiO_2 at 450 °C shows highest activity due to high crystallinity, and well-defined biporous mesostructure and surface area [22]. The mesostructure allows the reactant molecules to more

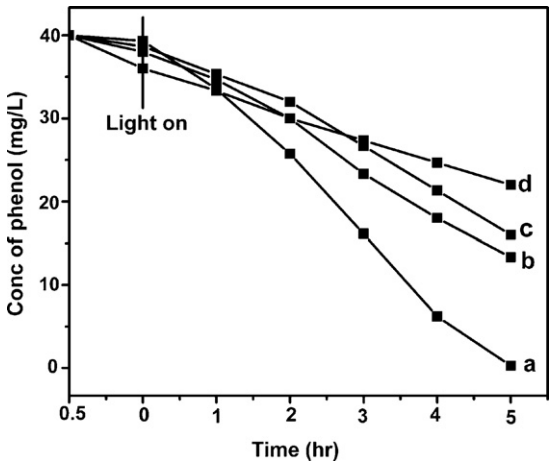

Fig. 9. Phenol degradation pathway using (a) MS-TiO_2, (b) with P123, (c) with PEG and (d) Degussa P25.

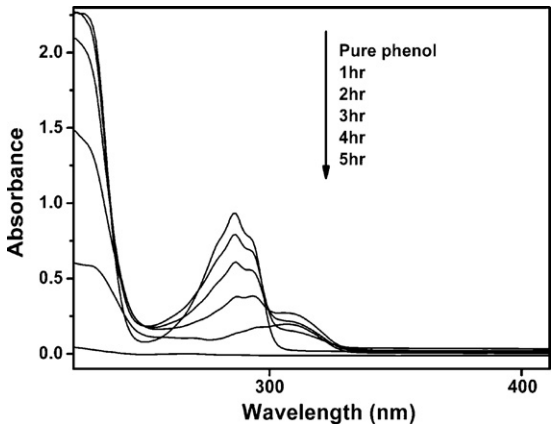

Fig. 10. Spectral changes during phenol degradation using MS-TiO_2 calcined at 450 °C.

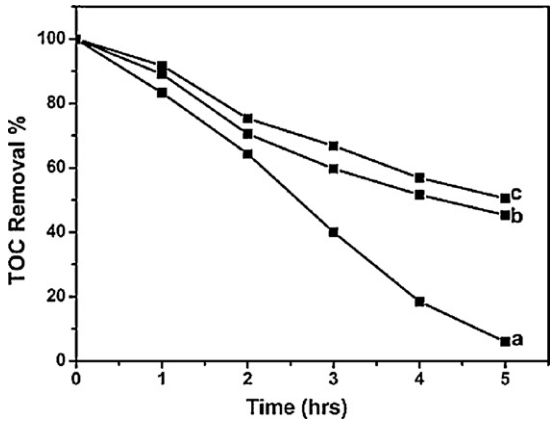

Fig. 11. TOC removal of phenol during degradation using different mesoporous TiO_2 calcined at 450 °C.

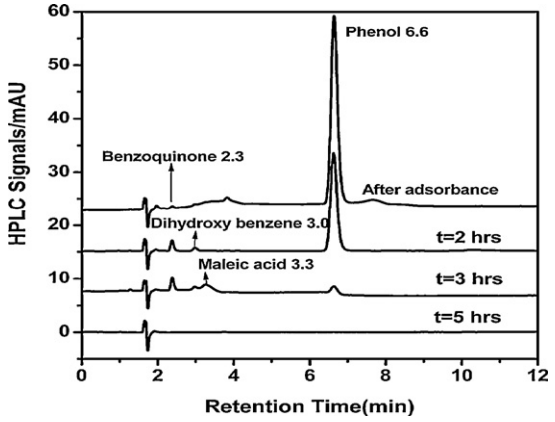

Fig. 12. HPLC changes during phenol degradation using MS-TiO_2 calcined at 450 °C.

readily access the active sites and provide the more pathways for the reactants to enter and products to escape [41]. The high crystallization of anatase facilitates the rapid transfer of photoelectrons from bulk to the surface, which can effectively inhibit the recombination between photoelectrons and holes, leading to enhanced quantum efficiency [42,43].

Absorbance spectrum of phenol degradation is shown in Fig. 10. It shows the main absorbance at 269 nm and another absorbance at λ 249 nm as well as a tailing absorbance with a shoulder in the region of λ 300–400 nm. The new absorbance is observed at λ 249 nm which is probably related to an intermediate degradation

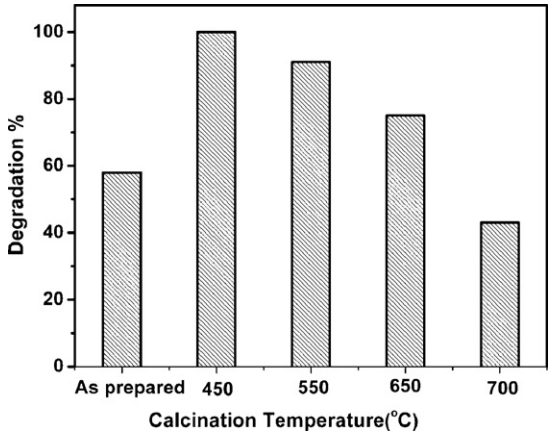

Fig. 13. Phenol degradation at different calcination temperatures using MS-TiO_2.

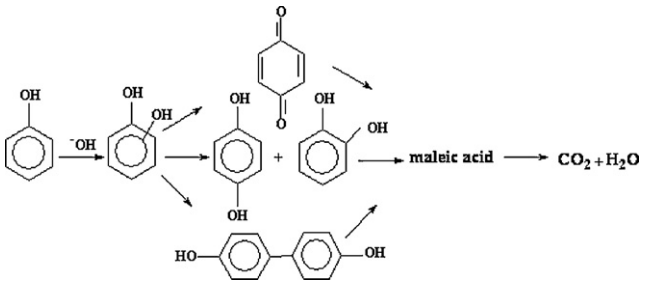

Scheme 2. Schematic representation of the degradation process of phenol.

product (presumably 4,4′-dihydroxybiphenyl) and the broad tailing absorption spectra are indicative of other aromatic degradation intermediates. After 5 h of irradiation, near complete mineralization of phenol is observed.

The mechanism for phenol degradation is proposed in Scheme 2 on the basis of HPLC results. The photocatalytic oxidation of phenol involves complicated multistage processes. It has been demonstrated that the photocatalytic process with TiO_2 is energetically favorable for the decomposition of phenolic compounds and that two types of oxidizing species hydroxyl radicals and positive holes are involved in the transformation of aromatic compounds in oxygenated aqueous TiO_2 suspensions [44]. Various aromatic intermediates products are formed in the initial stage. These intermediate products then undergo further photocatalytic oxidation to induce ring cleavage to form aliphatic acids and finally, they completely degrade to CO_2 and H_2O. Scheme 2 shows the detected intermediates of phenol degradation by HPLC data. By comparison of retention time with the standard components dihydroxybenzene (RT 3.0 min), benzoquinone (RT 2.3 min), 4,4′-dihydroxybiphenyl, and maleic anhydride (RT 3.3 min) are the main intermediates identified. Because no other intermediates (e.g., aliphatic acids) are observed, it appears that the intermediates mentioned above further degraded to more polar compounds such as carboxylic acid and eventually degraded to CO_2 [45]. The further degradation of the intermediates is likely via several reaction pathways (including oxidative hydroxylation, ring cleavage, oxidative decarboxylation, etc.) that are simultaneously operative. HPLC graph (Fig. 12) illustrated the removal of number of intermediates and phenol concentrations with the irradiation time. The photodegradation pathway proposed in Scheme 2 is consistent with the results of other research groups with anatase TiO_2 nanoparticles as catalyst [46].

4. Conclusions

New combination of P123 and PEG with acetic acid proved a suitable template system for preparation of mesoporous anatase with high crystallinity in the as prepared sample during the preparation method as compared to single templates system. MS-TiO_2 retained its mesoscale order up to 450 °C with highly crystalline anatase framework. MS-TiO_2 has higher thermal stability and biporous mesostructure. The pore properties were maintained up to 700 °C, which was attributed to the thermally stable anatase-nanocrystal framework. The catalytic activity of the MS-TiO_2 was much higher than that of the mesoporous TiO_2 prepared with single template and Degussa P25. The remarkably high catalytic activity of the MS-TiO_2 was derived from its high crystallinity and biporous mesostructure. The mesoporous structure could provide the more accessible site for pollutants and highly crystalline anatase enhance the quantum efficiency. This work provides a new pathway to design and fabricate novel photoactive materials for catalyst and other applications.

Acknowledgments

This work has been supported by National Nature Science Foundation of China (20773039, 20977030), National Basic Research Program of China (973 Program, 2007CB613301, 2010CB732306), Science and Technology Commission of Shanghai Municipality (10520709900, 10JC1403900) and the Fundamental Research Funds for the Central Universities. Shamaila Sajjad and Sajjad Ahmed Khan Leghari would like to thank Higher Education Commission of Pakistan for financial support.

References

[1] C.T. Kresge, M.E. Leonowicz, W.J. Roth, J.C. Vartuli, J.S. Beck, Nature 359 (1992) 710–712.
[2] C.-W. Koh, U.-H. Lee, J.-K. Song, H.-R. Lee, M.-H. Kim, M. Suh, Y.-U. Kwon, Asian J. Chem. 3 (2008) 862–867.
[3] L. Zhang, Y. Zhu, Y. He, W. Li, H. Sun, Appl. Catal. B: Environ. 40 (2003) 287–292.
[4] H. Zhao, D. Jiang, S. Zhang, W. Wen, J. Catal. 250 (2007) 102–109.
[5] S. Shamaila, A.K.L. Sajjad, F. Chen, J. Zhang, Chem. Eur. J. 16 (2010) 13795–13804.
[6] J. Zhang, Y. Wu, M. Xing, S.A.K. Leghari, S. Sajjad, Energy Environ. Sci. 3 (2010) 715–726.
[7] S. Yuan, Q. Sheng, J. Zhang, F. Chen, M. Anpo, Q. Zhang, Micropor. Mesopor. Mater. 79 (2005) 93–99.
[8] P. Puhlfurb, A. Voigt, R. Weber, M. Morb, J. Membr. Sci. 174 (2000) 123–133.
[9] S. Shamaila, A.K.L. Sajjad, F. Chen, J. Zhang, Appl. Catal. B: Environ. 94 (2010) 272–280.
[10] S. Shamaila, A.K.L. Sajjad, F. Chen, J. Zhang, Mater. Res. Bull. 45 (2010) 1372–1382.
[11] S. Hirobumi, O. Taku, M. Tatsuya, O. Takahiro, S. Hideki, A. Masahiko, J. Am. Chem. Soc. 127 (2005) 16396–16397.
[12] B. Smarsly, D. Grosso, T. Brezesinski, N. Pinna, C. Boissiere, M. Antonietti, C. Sanchez, Chem. Mater. 16 (2004) 2948–2952.
[13] J. Lee, M.C. Orilall, S.C. Warren, M. Kamperman, F.J. DiSalvo, U. Wiesner, Nat. Mater. 7 (2008) 222–228.
[14] H. Yoshitake, T. Sugihara, T. Tatsumi, Chem. Mater. 14 (2002) 1023–1029.
[15] K. Cassiers, T. Linssen, M. Mathieu, Y.Q. Bai, H.Y. Zhu, P. Cool, E.F. Vansant, J. Phys. Chem. B 108 (2004) 3713–3721.
[16] S. Yuan, Q. Sheng, J. Zhang, F. Chen, M. Anpo, W. Dai, Catal. Lett. 107 (2006) 19–24.
[17] J.C. Yu, L. Zhang, J. Yu, Chem. Mater. 14 (2002) 4647–4653.
[18] P.C.A. Alberius, K.L. Frindell, R.C. Hayward, E.J. Kramer, G.D. Stucky, B.F. Chmelka, Chem. Mater. 14 (2002) 3284–3294.
[19] B.T. Holland, L. Abrams, A. Stein, J. Am. Chem. Soc. 121 (1999) 4308–4309.
[20] T. Sen, G.J.T. Tiddy, J.L. Casci, M.W. Anderson, Chem. Mater. 16 (2004) 2044–2054.
[21] J.H. Sun, Z. Shan, T. Maschmeyer, M.O. Coppens, Langmuir 19 (2003) 8395–8402.
[22] M. Groenewolt, M. Antoneitti, S. Ploarz, Langmuir 20 (2004) 7811–7819.
[23] Q. Sheng, Y. Cong, S. Yuan, j. Zhang, M. Anpo, Micropor. Mesopor. Mater. 95 (2006) 220–225.
[24] J.H. Smatt, S. Schunk, M. Linden, Chem. Mater. 15 (2003) 2354–2361.
[25] S. Bu, Z. Jin, X. Liu, L. Yang, Z. Cheng, Mater. Chem. Phys. 88 (2004) 273–279.
[26] J.C. Yu, L. Zhang, J. Yu, New J. Chem. 26 (2002) 416–420.
[27] X.J. Ding, T.C. An, G.Y. Li, S.Q. Zhang, J.X. Chen, J.M. Yuan, H.J. Zhao, H. Chen, G.Y. Sheng, J.M. Fu, J. Colloid Interface Sci. 320 (2008) 501–507.
[28] P. Feng, X. Bu, D. Pine, Langmuir 16 (2000) 5304–5310.
[29] P.D. Yang, D.Y. Zhao, D.I. Margolese, B.F. Chmelka, G.D. Stucky, Nature 396 (1998) 152–155.
[30] J.L. Blin, A. Leonard, Z.Y. Yuan, L. Gigot, A. Vantomme, A.K. Cheetham, B.L. Su, Angew. Chem., Int. Ed. 42 (2003) 2872–2875.
[31] D. Grosso, G.J.A.A. Soler-Illia, F. Babonneau, C. Sanchez, P.A. Albouy, A. Brunet-Bruneau, A.R. Balkenende, Adv. Mater. 13 (2001) 1085–1090.
[32] S.Y. Choi, M. Mamak, N. Coombs, N. Chopra, G.A. Ozin, Adv. Funct. Mater. 14 (2004) 335–344.
[33] B. Wen, C. Liu, Y. Liu, J. Photochem. Photobiol. A: Chem. 173 (2005) 7–12.
[34] X.H. Hu, T.C. An, M.L. Zhang, G.Y. Sheng, J.M. Fu, Res. J. Chem. Environ. 11 (2007) 13–21.
[35] G.V. Vasilenko, V.I. Zarembo, A. Slobodov, A. Russ, J. Appl. Chem. 70 (1997) 1498–1500.
[36] J. Yang, J.M.F. Ferreira, Mater. Lett. 36 (1998) 320–324.
[37] C. Liu, L. Fub, J. Economy, J. Mater. Chem. 14 (2004) 1187–1189.
[38] K.S. Yoo, T.G. Lee, J. Kim, Micropor. Mesopor. Mater. 84 (2005) 211–217.
[39] X. Wang, J.C. Yu, C. Ho, Y. Hou, X. Fu, Langmuir 21 (2005) 2552–2559.
[40] D.W. Lee, S.J. Park, S.K. Ihm, K.H. Lee, Chem. Mater. 19 (2007) 937–941.
[41] S.S. Kim, T.R. Pauly, T.J. Pinnavaia, Chem. Commun. 10 (2000) 835–836.
[42] M.R. Hoffmann, S.T. Martin, W.Y. Choi, D.W. Bahnemannt, Chem. Rev. 95 (1995) 69–96.
[43] A. Fujishima, T.N. Rao, D.A. Tryk, J. Photochem. Photobiol. C 1 (2000) 1–21.
[44] K. Nagaveni, G. Sivalingam, M.S. Hegde, G. Madras, Environ. Sci. Technol. 38 (2004) 1600–1604.
[45] M. Salaices, B. Serrano, H.I. De-Lasa, Chem. Eng. Sci. 59 (2004) 3–15.
[46] E.B. Azevedo, F.R. Aquino Neto, M. Dezotti, Appl. Catal. B: Environ. 54 (2004) 165–173.